Protein Science (1993), *2*, 93–102. Cambridge University Press. Printed in the USA.

Increasing nitrogenase catalytic efficiency for MgATP by changing serine 16 of its Fe protein to threonine: Use of Mn^{2+} to show interaction of serine 16 with Mg^{2+}

LANCE C. SEEFELDT AND LEONARD E. MORTENSON
Biochemistry Department, University of Georgia, Athens, Georgia 30602

(RECEIVED August 13, 1992; REVISED MANUSCRIPT RECEIVED September 18, 1992)

Abstract

MgATP-binding and hydrolysis are an integral part of the nitrogenase catalytic mechanism. We are exploring the function of MgATP hydrolysis in this reaction by analyzing the properties of the Fe protein (FeP) component of *Azotobacter vinelandii* nitrogenase altered by site-directed mutagenesis. We have previously (Seefeldt, L.C., Morgan, T.V., Dean, D.R., & Mortenson, L.E., 1992, *J. Biol. Chem. 267*, 6680–6688) identified a region near the N-terminus of FeP that is involved in interaction with MgATP. This region of FeP is homologous to the well-known nucleotide-binding motif GXXXXGKS/T. In the present work, we examined the function of the four hydroxyl-containing amino acids immediately C-terminal to the conserved lysine 15 that is involved in interaction with the γ-phosphate of MgATP. We have established, by altering independently Thr 17, Thr 18, and Thr 19 to alanine, that a hydroxyl-containing residue is not needed at these positions for FeP to function. In contrast, an hydroxyl-containing amino acid at position 16 was found to be critical for FeP function. When the strictly conserved Ser 16 was altered to Ala, Cys, Asp, or Gly, the FeP did not support N_2 fixation when expressed in place of the wild-type FeP in *A. vinelandii*. Altering Ser 16 to Thr (S16T), however, resulted in the expression of an FeP that was partially active. This S16T FeP was purified to homogeneity, and its biochemical examination allowed us to assign a catalytic function to this hydroxyl group in the nitrogenase mechanism. Of particular importance was the finding that the S16T FeP had a significantly higher affinity for MgATP than the wild-type FeP, with a measured K_m of 20 μM compared to the wild-type FeP K_m of 220 μM. This increased kinetic affinity for MgATP was reflected in a significantly stronger binding of the S16T FeP for MgATP. In contrast, the affinity for MgADP, which binds at the same site as MgATP, was unchanged. The catalytic efficiency (k_{cat}/K_m) of S16T FeP was found to be 5.3-fold higher than for the wild-type FeP, with the S16T FeP supporting up to 10 times greater nitrogenase activity at low MgATP concentrations. This indicates a role for the hydroxyl group at position 16 in interaction with MgATP but not MgADP. The site of interaction of this residue was further defined by examining the properties of wild-type and S16T FePs in utilizing MnATP compared with MgATP. The S16T FeP was severely compromised in its interaction with MnATP, suggesting a mechanism where the hydroxyl group of amino acid 16 interacts with the Mg^{2+} of bound MgATP.

Keywords: Fe protein; mechanism; MgADP; MgATP; MnATP; MoFe protein; mutagenesis; nitrogenase

Nitrogenase catalyzes the hydrolysis of about 16 MgATP to 16 MgADP + 16 Pi for each N_2 that is reduced to 2 NH_3. The function of MgATP hydrolysis in this reduction is not established. Nitrogenase is a two component enzyme that consists of a tetrameric MoFe protein (MoFeP), with two 8Fe (Bolin et al., 1990) and two MoFeS centers (FeMoco) and a homodimeric Fe protein (FeP) that contains one 4Fe–4S cluster bridging its subunits (Hausinger & Howard, 1983; Howard et al., 1989; Georgiadis et al., 1990). The MoFeS clusters of MoFeP are thought to be the site of N_2 binding and reduction. One of the functions of the FeP is to transfer a low potential electron from reduced flavodoxin to the MoFeP (suggested to be its 8Fe center) for use in the reduction

Reprint requests to: Leonard E. Mortenson, Biochemistry Department, University of Georgia, Athens, Georgia 30602.

Abbreviations: FeP, iron protein; MoFeP, molybdenum-iron protein; FeP_{Av}, iron protein from *Azotobacter vinelandii*; SDS, sodium dodecyl sulfate.

of N_2. This electron transfer step is only one function of the FeP, however, because the MoFeP alone will not reduce N_2 without the FeP, despite the fact that the MoFeP component can be reduced by other electron sources (Burgess, 1990). This second, major function of the FeP is intimately related to the need for MgATP hydrolysis during nitrogenase catalysis. Only the complex of MoFeP, reduced FeP, and MgATP results in the hydrolysis of MgATP and the transfer of an electron. However, the FeP alone can bind two MgATP per dimer, undergoing a conformational change that affects several of its properties, including the midpoint potential of its 4Fe-4S center (Zumft et al., 1974; Morgan et al., 1986) and its ability to interact with the MoFeP (Seefeldt et al., 1992). Kinetic evidence suggests that following each electron transfer step, oxidized FeP·$(MgADP)_2$ dissociates from the partially reduced MoFeP, which then associates with another reduced FeP·$(MgATP)_2$ to effect a second one-electron transfer (Hageman & Burris, 1978; Lowe & Thorneley, 1984). Subsequent rounds of MgATP hydrolysis and electron transfer result in the eventual accumulation of sufficient electrons to reduce N_2 to NH_3.

In an attempt to better understand the role of MgATP hydrolysis in nitrogenase catalysis, we are systematically analyzing the properties of FePs from *Azotobacter vinelandii* (FeP_{Av}), which are altered by means of site-directed mutagenesis. In a recent paper (Seefeldt et al., 1992), we identified a region of the FeP_{Av} that is involved in its interaction with MgATP. This region is located near the N-terminus of the FeP and is similar to the motif in other nucleotide-binding proteins (GXXXXGKS/T) that is involved in binding the phosphate groups of nucleotides (Walker et al., 1982; Saraste et al., 1990). We demonstrated that the conserved lysine of this motif (Lys 15 of FeP_{Av}) plays a major role in the interaction of FeP_{Av} with the γ-phosphate group of MgATP and is critical for the coupling of nucleotide binding to the conformational change of the FeP that is essential for its interaction with the MoFeP. In the present work, we have altered the four amino acids immediately C-terminal to this critical Lys 15, namely Ser 16, Thr 17, Thr 18, and Thr 19. We now show that at position 16, an amino acid with a hydroxyl side chain is required for FeP to function, and we suggest that this hydroxyl group is associated with the Mg^{2+} of the bound MgATP.

Results

Site-directed mutagenesis of FeP_{Av}

Figure 1 compares the amino acid sequence of FeP_{Av} adjacent to the conserved Lys 15 of the phosphate-binding domain with the conserved amino acid consensus sequences for all FePs and with the corresponding amino acids for several other families of nucleotide-binding proteins. In most of the families shown, there is either a conserved serine or threonine adjacent to the conserved lysine. In several of the families (e.g., elongation factors, ras p21, and thymidine kinase) both serine and threonine are found and often appear to be used interchangeably. In all FePs for which sequences are known (22 in total), only serine is found at the position equivalent to 16 of FeP_{Av} (Normand & Bousquet, 1989). In the next three positions, hydroxyl-containing amino acids are common among these families, although not universally conserved. In all FePs, threonine is conserved next to the conserved serine and is often, but not always, followed by two more hydroxyl amino acids. In the case of FeP_{Av} three threonine residues follow the conserved serine (Thr 17, 18, and 19). In light of (1) the high degree of conservation of the amino acids in this region among different nucleotide-binding proteins, (2) their proximity to the lysine which plays a major role in MgATP interaction in FeP and other nucleotide-binding proteins, and (3) evidence from X-ray structures of several nucleotide-binding proteins with bound nucleotides that suggest that this region is involved with phosphate binding (Pai et al., 1990; Kjeldgaard & Nyborg, 1992; Muller & Schulz, 1992), we have changed each of these amino acids individually in FeP_{Av} to gain insights into the mechanism of MgATP hydrolysis by nitrogenase.

	15	16	17	18	19
A. vinelandii FeP	G	K	S	T	T	T
FeP consensus	g	K	S	T	t	s
Elongation factors	G	K	S/T	T	t	t
Ras P-21	G	K	S/T	a	L	t
Thymidine kinase	g	K	S/T	t	t	l
ATP synthase-β	G	K	T	V	l	i
Myosin	G	K	T	e	n	S/T
Adenylate kinase	G	K	G	T	q	c

Fig. 1. Conserved hydroxyl-containing amino acids in the phosphate-binding domain of nitrogenase Fe proteins and other nucleotide-binding proteins. Strictly conserved amino acids are presented as uppercase letters, and nonconserved, consensus amino acids are presented as lowercase letters. The FeP consensus was derived from the sequences of 22 different FePs (Normand & Bousquet, 1989). The consensus sequences for the other nucleotide-binding proteins were derived from Saraste et al. (1990). The numbering at the top refers to the amino acid position for *Azotobacter vinelandii* FeP.

Table 1 lists the amino acid changes that were made in FeP_{Av} and the phenotypes of *A. vinelandii* cells expressing each of the altered proteins in place of the wild-type FeP. When each of the threonine residues, Thr 17, Thr 18, and Thr 19, were changed individually to either serine or alanine, the resulting cells grew under N_2-fixing conditions at either the same rate as wild-type cells or at an even greater rate. The good N_2-fixing activity of cells expressing T(17, 18, or 19)A FeP reveals that a hydroxyl-containing amino acid at these positions individually is not essential for the FeP to function in vivo. In contrast to these three residues, changing the conserved serine at po-

Table 1. *Summary of FeP mutants and phenotypes*

Position altered	Phenotype[a]	Doubling time (h)[b]
Wild type	+	3.6 (100%)
S16		
T	+	8.7 (41%)
A	−	n.g.
D	−	n.g.
G	−	n.g.
C	−	n.g.
T17		
S	+	4.0 (90%)
A	+	3.6 (100%)
T18		
S	+	3.7 (97%)
A	+	3.1 (116%)
T19		
S	+	3.3 (108%)
A	+	2.8 (128%)

[a] + indicates that the cells are able to grow by fixing N_2 as their sole source of nitrogen; − indicates that the cells are not able to grow on N_2 (see Materials and methods for growth conditions).

[b] Doubling times are for liquid cultures growing in the absence of fixed nitrogen; n.g. indicates no growth. Numbers in parentheses represent percentage of wild-type doubling times.

sition 16 to the non-hydroxyl-containing residues alanine, aspartic acid, glycine, or cysteine resulted in FePs that were nonfunctional in vivo. Replacement of the conserved S16 with threonine in FeP resulted in cells that could still fix N_2, although at 41% of the rate of cells with serine at that position. Because at position 16 of FeP_{Av}, threonine but not alanine or cysteine supported N_2 fixation, our data strongly suggest that a hydroxyl group at position 16 is essential for FeP function. As noted above, whereas in most nucleotide-binding proteins threonine and serine residues can be found at this position, among 22 different FePs only serine is found. We examined the properties of the FeP_{Av} from S16T cells to probe the mechanism of this residue in FeP.

S16T FeP

Homogeneous S16T FeP was purified from derepressed *A. vinelandii* cells with a yield of 250 mg of S16T FeP from 100 g of wet cells. This contrasts sharply with our typical yield of 75 mg of wild-type FeP from 100 g of wet cells. Because the synthesis of nitrogenase is known to be repressed by the presence of ammonia in the cell growth media (and within cells), the higher yield of nitrogenase found in the slower-growing S16T cells probably results from the facts that (1) nitrogen is limiting and the lower rate of N_2 fixation in S16T does not allow ammonia to accumulate and control nitrogenase biosynthesis, and (2) the modified nitrogenase is still active and produces sufficient ammonia to support the synthesis of high concentrations of nitrogenase. This latter point would not be true of mutants with inactive FeP. The S16A, S16D, and S16G FePs, although normally expressed in whole cells following nitrogen derepression as determined by denaturing gel electrophoretic analysis of lysed whole cells, could not be purified in quantities sufficient for analysis. This suggests that these latter proteins might be unstable as a result of the amino acid change.

Activities of S16T FeP

The nitrogenase activity of S16T FeP complexed with wild-type MoFeP (S16T FeP·MoFeP) was compared with that of the wild-type FeP·MoFeP complex in a variety of reactions known to monitor different nitrogenase activities. During N_2 reduction by either whole cells or purified nitrogenase, two H^+ are reduced to form one H_2 for each N_2 that is reduced to form two NH_3. It is believed that this H_2 evolution reaction is an integral part of the N_2 fixation mechanism with the total rate of electron flux being the sum of rates of H^+ and N_2 reduction. Under conditions of low N_2, nitrogenase only reduces H^+, such that the total rate of electron flux now can be measured as the rate of H_2 production. In addition, nitrogenase reduces acetylene to ethylene (Dilworth, 1966) with little production of H_2, thus providing another way to monitor the total flow of electrons through nitrogenase. Still another way to follow nitrogenase activity is by measuring electron-dependent hydrolysis of MgATP. Under ideal conditions, two MgATP are hydrolyzed to two MgADP for each electron that is transferred to substrate and therefore four MgATP are hydrolyzed for each H_2 evolved or for each acetylene reduced to ethylene. In vitro, the measured rate of MgATP hydrolysis during nitrogenase catalysis is lower than expected because the MgADP that is generated during the course of the reaction competitively inhibits further MgATP hydrolysis. Table 2 lists the specific activities of wild-type and S16T FePs for each of the reactions described above coupled to wild-type MoFeP. As can be seen, N_2 reduction, H_2 evolution and C_2H_2 reduction for the S16T FeP·MoFeP complex all were 32–41% of that observed for the wild-type FeP·MoFeP complex. These percentages are similar to the 40% N_2-fixing growth rate of *A. vinelandii* cells containing S16T FeP (Table 1) when compared to the wild-type cells. The MgATP hydrolysis rate of the S16T FeP·MoFeP complex was found to be 49% of that of wild-type FeP·MoFeP complex. This slightly higher rate compared to the substrate reduction rates suggests that there is a slight uncoupling of MgATP hydrolysis from electron transfer for the S16T FeP.

Interaction of S16T FeP with MoFeP

Because of the reduced activities of S16T FeP when associated with MoFeP, we designed experiments to exam-

Table 2. *Activities of wild-type and S16T nitrogenase Fe proteins*

Activity[a]	Specific activity	
	Wild-type FeP	S16T FeP[b]
N_2 reduction (nmol NH_3 min^{-1} mg^{-1})	1,026 ± 39	324 ± 12 (32%)
Acetylene reduction (nmol C_2H_4 min^{-1} mg^{-1})	1,964 ± 51	705 ± 19 (36%)
H_2 evolution (nmol H_2 min^{-1} mg^{-1})	2,394 ± 56	972 ± 22 (41%)
MgATP hydrolysis (nmol MgADP min^{-1} mg^{-1})	6,009 ± 119	2,969 ± 56 (49%)

[a] Specific activities were determined as described in the Materials and methods. All activities are per milligram of FeP.
[b] Numbers in parentheses are percent activities relative to wild type.

ine the reasons for this. One possibility was that the substitution of threonine at position 16 resulted in a change in the protein that affected its ability to interact with the MoFeP. To address this, we examined the apparent affinity of the wild-type and S16T FePs for MoFeP using the FeP titration experiment described (Wolle et al., 1992). In this experiment, a fixed amount of MoFeP is titrated with increasing amounts of FeP. It is assumed that the FeP behaves like a simple substrate in the nitrogenase reaction, such that a plot of activity versus increasing substrate (FeP) concentration should yield a substrate saturation plot. From this plot, an apparent binding constant (K_mAvII) for FeP binding to MoFeP can be determined as the concentration of FeP that yields half the maximal rate. Figure 2 shows that S16T FeP binds tighter to MoFeP, with a K_mAvII of <0.2 μM, compared to a K_mAvII of WT FeP of 0.6 μM. Thus, it is possible that

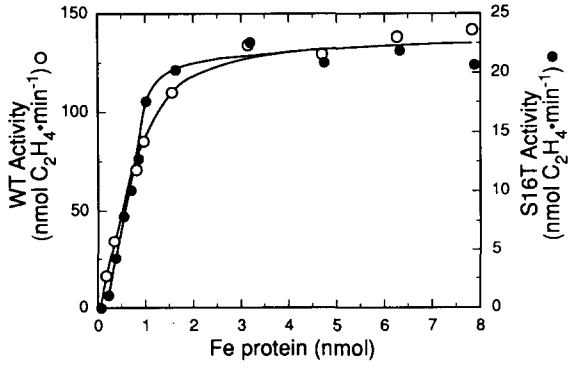

Fig. 2. Dependence of nitrogenase actylene reduction activity on the concentration of wild-type or S16T Fe protein. Acetylene reduction activity under low salt conditions was determined as described in the Materials and methods. Assay liquid volumes were 1 mL. Each assay contained 64 mg of wild-type MoFeP and the indicated concentrations of either wild-type (O) or S16T (●) FeP.

the lower activity for S16T FeP compared to WT FeP at high MgATP concentrations results from tighter binding to the MoFeP.

Interaction of S16T FeP with MgATP and MgADP

Because the serine at position 16 is adjacent to the lysine 15 that we have shown interacts with the γ-phosphate of MgATP, we performed several experiments to examine the likely possibility that serine at position 16 also interacts with MgATP. Figure 3A shows the dependence of nitrogenase activity on increasing MgATP concentration for both the wild-type FeP·MoFeP complex and the S16T FeP·MoFeP complex. From the data, it is obvious that changing serine 16 of FeP_{Av} to threonine dramatically alters the dependence of the nitrogenase complex on the MgATP concentration. In particular, it can be seen that whereas wild-type FeP achieves a higher maximum activity than the S16T FeP at high MgATP concentrations, S16T FeP reaches a higher maximum rate than wild-type FeP at lower MgATP concentrations (Fig. 3B). A comparison of the "affinity" of the two nitrogenases for MgATP, estimated from their apparent K_m's for MgATP, showed an apparent K_m of 220 μM for the wild-type FeP, a value comparable to that observed by others (Yates, 1991), and of 20 μM for S16T FeP. In this comparison, the S16T FeP has an 11-fold increased affinity for MgATP. These values, together with the k_{cat} for MgATP hydrolysis for S16T and wild-type FePs, along with their catalytic efficiencies (k_{cat}/K_m), are summarized in Table 3. Substitution of serine 16 for threonine in FeP results in a 5.3-fold increase in the catalytic efficiency of nitrogenase for MgATP. One can see from the data in Figure 3 that at low MgATP concentrations apparent cooperativity of MgATP use exists, although this was similar for both the S16T FeP and wild-type FeP.

The data above conclusively show that changing the serine 16 of FeP to threonine has affected the interaction of the nitrogenase complex with MgATP. Specifically, the S16T protein has a 2-fold lower k_{cat} and an 11-fold lower K_m. Because FeP itself binds MgATP and because our results in Table 3 show a large difference in the K_m val-

Table 3. *Interaction of S16T and wild-type FeP with MgATP*

FeP	MgATP K_m (μM)	MgATP k_{cat} (min^{-1})	MgATP catalytic efficiency k_{cat}/K_m (μM^{-1} min^{-1})	Ratio of MgATP catalytic efficiency S16T/WT
Wild type	220	385.2	1.8	5.3
S16T	20	190.3	9.5	

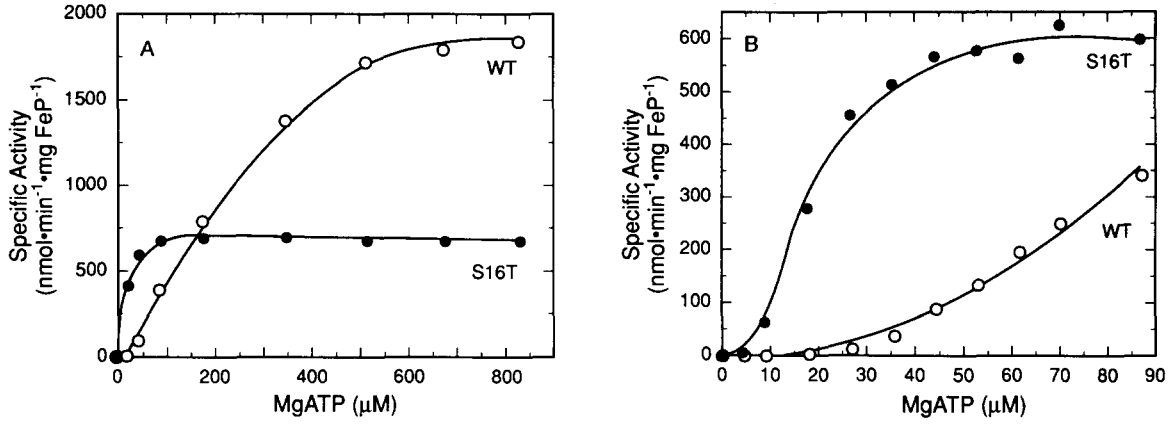

Fig. 3. Dependence of nitrogenase acetylene reduction activity on MgATP concentration for wild-type and S16T Fe proteins. Acetylene reduction activity was determined as described in the Materials and methods. Each assay vial contained 276 mg of wild-type MoFeP and 125 mg of either wild-type (WT) (○) or S16T (●) FeP. ATP concentration was varied by adding different volumes of a stock ATP solution. **A:** A broad MgATP concentration range. **B:** The conditions under low MgATP concentration. The MgATP concentration required to achieve half-maximal activity was taken as the apparent K_m for MgATP and corresponds to 220 μM for wild-type FeP and 20 μM for S16T FeP.

ues, we compared the binding of MgATP to S16T FeP and wild-type FeP. When monitored directly by an equilibrium-binding assay previously described (Bui & Mortenson, 1968), we found that under identical conditions wild-type FeP bound 0.2 MgATP/FeP (Fig. 4A) and S16T FeP bound 1.4 MgATP/FeP (Fig. 4B). A subsaturating concentration of MgATP was used in these experiments to allow maximum detection of differences in "affinity" between the two FePs. This result reveals that the 11-fold lower K_m (MgATP) for S16T FeP in the nitrogenase reaction results from the substantial increase in the S16T FeP's "affinity" for MgATP.

In addition to MgATP, FeP also binds MgADP, the product of MgATP hydrolysis. MgADP binding to FeP is competitive with MgATP, indicating that these two species interact at the same site on the protein (Moustafa & Mortenson, 1967). Using the same equilibrium binding assay we used for MgATP-binding, we found that both wild-type and S16T FePs bound MgADP with nearly identical affinities (Fig. 5), with ratios of 1.63 MgADP/wild-type FeP and 1.57 MgADP/S16T FeP. We conclude, therefore, that the hydroxyl group at position 16 interacts with MgATP but not with MgADP.

Unlike the K15Q FeP (Seefeldt et al., 1992), the S16T FeP was found to undergo the MgATP-induced conformational change that results in the rhombic-to-axial EPR change and the chelation of Fe^{2+} from the cluster by α,α'-dipyridyl just as for wild-type FeP.

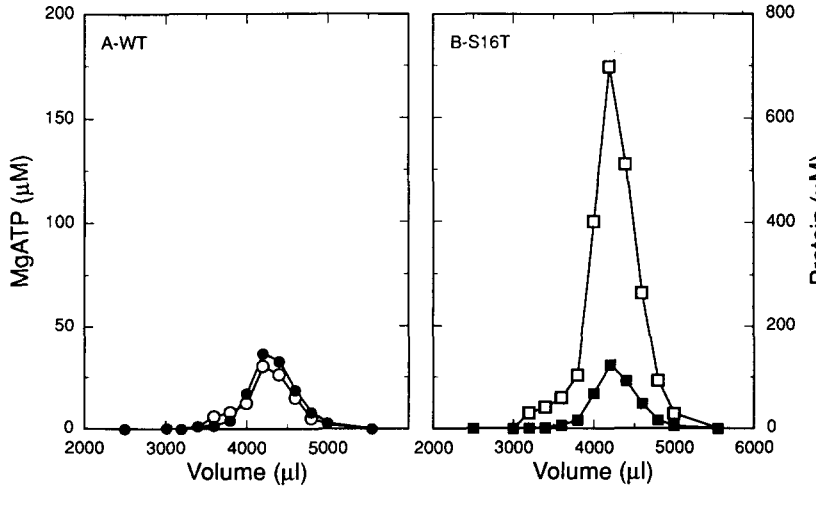

Fig. 4. MgATP binding to wild-type and S16T Fe protein. Equilibrium column binding of MgATP to purified FeP was performed as described in the Materials and methods. **A:** Wild-type (WT) FeP. **B:** S16T FeP. Open symbols (○, □) are the MgATP concentration and closed symbols (●, ■) are the protein concentration in each column fraction.

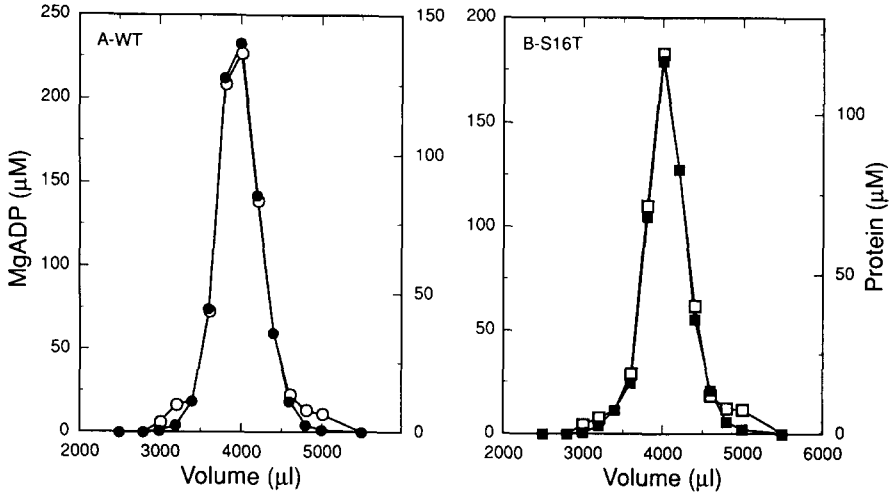

Fig. 5. MgADP binding to wild-type and S16T Fe protein. Conditions are as described in Figure 4, except that the buffer contains MgADP instead of MgATP. **A:** Wild-type FeP. **B:** S16T FeP. Open symbols (○, □) are the MgADP concentration, and closed symbols (●, ■) are the protein concentration in each column fraction.

Probing the site of interaction of the position 16 hydroxyl by use of the divalent metal ions Mg^{2+} and Mn^{2+}

FeP will only interact with ATP or ADP when they are chelated with a divalent metal ion. Although the preferred metal ion is Mg^{2+}, nitrogenase also will function with MnATP (Burns, 1969), but at a lower rate. We have taken advantage of the differential effects of the two counter ions to further probe the site of interaction of the position 16 hydroxyl. Figure 6A shows how wild-type FeP·MoFeP activity responds to increasing concentrations of the counter ions, Mg^{2+} or Mn^{2+}. Figure 6B shows how S16T FeP·MoFeP activity responds under the same conditions. Although both FePs respond similarly to Mg^{2+}, there is a dramatic difference in the responses of the two nitrogenase complexes to Mn^{2+}. Specifically, S16T FeP uses Mn^{2+} as a counterion very poorly (Fig. 6B). This extremely low rate with Mn^{2+} is well below the predicted rate (dashed line in Fig. 6B) for the S16T FeP·MoFe complex calculated from the differences seen with Mg^{2+} suggesting Mg^{2+} on MgATP as the site of interaction of the hydroxyl at position 16 of FeP.

Discussion

The results presented in this work strongly support the suggestion that the γ-OH group of serine 16 of FeP interacts with the Mg^{2+} of bound MgATP. Hydroxyl groups at the three positions C-terminal to this residue (positions 17, 18, and 19) are not essential for FeP activity, although slightly increased cell growth resulted when mutants containing alanine in place of either threonine 18 or 19 were examined. The latter suggests that alanine in either position 18 or 19 provides a preferred secondary structure for the function of the FeP. In contrast, an OH-containing group at position 16 is an absolute requirement for FeP function and nitrogen-fixing cell growth. A comparison of properties of the wild-type and S16T FePs has provided clues to the role of the γ-OH group at this position. Of particular importance is the finding that S16T FeP binds MgATP with a much greater affinity than the wild-type FeP. This results in an FeP that is up to 10 times more active than wild-type FeP at low MgATP concentrations (10–70 μM) but which is less active at higher MgATP concentrations (>200 μM). Furthermore, a comparison of the k_{cat}/K_m for MgATP of the two FePs shows that the S16T FeP has a 5.3-fold higher catalytic efficiency than the wild-type FeP.

The role of S16 in MgATP hydrolysis

Based on these results, we have constructed a model for the role of the γ-OH group at position 16 in the mechanism of MgATP hydrolysis by nitrogenase (Fig. 7). Because nitrogenase hydrolyzes MgATP with no evidence for an intermediate phosphorylation step, it is reasonable to assume that a water molecule is the nucleophile that attacks the γ-phosphate of MgATP (Walsh, 1979). This H_2O could be activated for attack by a general base on the protein (e.g., a glutamic acid). Because we know that the FeP alone will not hydrolyze MgATP, we suggest that this residue may come from the MoFeP, and because it would only be available when the two components associate, FeP alone would not be expected to hydrolyze MgATP. Our previous work with lysine 15 (Seefeldt et al., 1992) would place the epsilon amino group of lysine in position to complex with the γ-phosphate group of MgATP. The free electron pair on the γ-OH group of serine 16 would be in a position to stabilize the Mg^{2+} of the bound MgATP. It is accepted that Mg^{2+} is bound to the β- and γ-phosphates of MgATP and to the α- and β-phosphates of MgADP (Cohn & Hughes, 1962). Thus, when the γ-phosphate of ATP is cleaved, it is necessary for the Mg^{2+} to shift to the α- and β-phosphates of the resulting product, ADP. In so doing, one would predict a transition

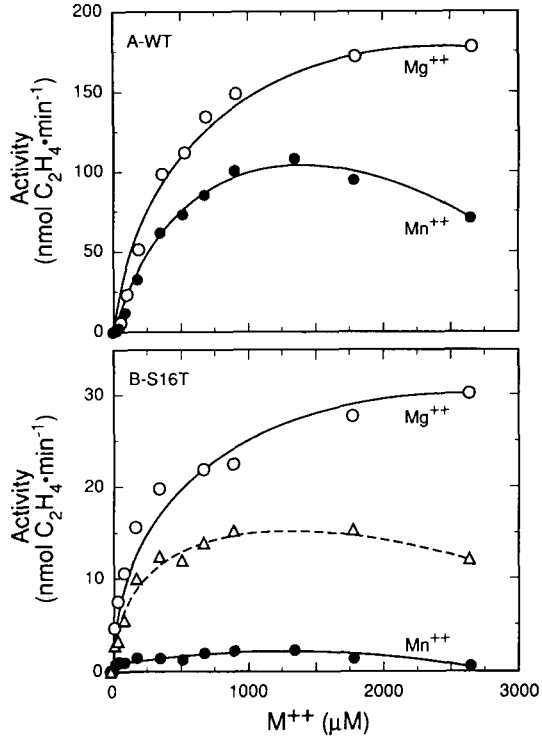

Fig. 6. Dependence of nitrogenase acetylene reduction activity on the concentration of the divalent metal ions Mg^{2+} or Mn^{2+} for wild-type and S16T Fe proteins. Acetylene reduction activity under low salt conditions was determined as described in the Materials and methods. Each assay contained 266 mg MoFeP and 125 mg of either **(A)** wild-type or **(B)** S16T FeP. M^{++} represents the concentration of Mg^{2+} (○) or Mn^{2+} (●). The open triangles (△) represent the predicted activity for S16T with Mn^{2+} as the divalent metal. This was calculated at each metal concentration by dividing the activity of wild-type FeP for Mn^{2+} by the Mg^{2+} activity and multiplying the resultant by the measured Mg^{2+} activity for S16T to yield the predicted Mn^{2+} activity for S16T FeP. The actual measured Mn^{2+}-dependent activity for S16T is represented by ●.

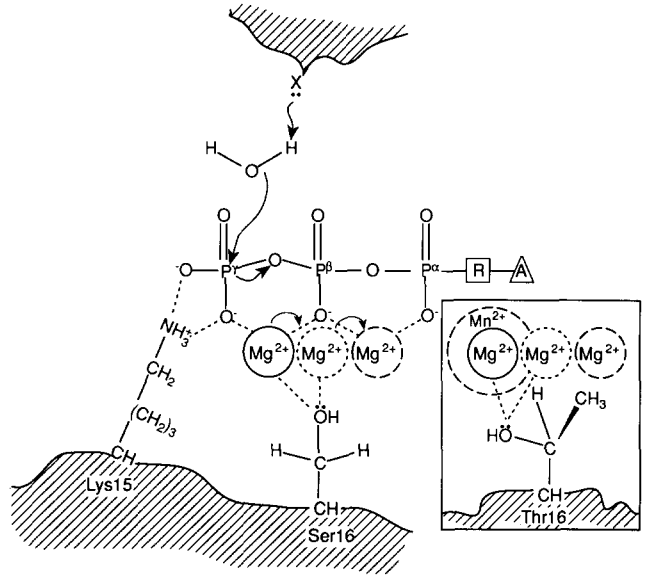

Fig. 7. Model for the role of lysine 15 and serine 16 of Fe protein in nucleotide hydrolysis. Adenine is represented by an A inside a triangle, and ribose is represented by an R inside a box. The transition state is represented by the dotted circle around the Mg^{2+}.

state in which the Mg^{2+} is bound predominantly to the β-phosphate of ATP and to the γ-OH of Ser 16. Thus, in this model, the γ-OH group of Ser 16 would act to partially stabilize the substrate, MgATP, by binding to the Mg^{2+} but would play an even greater role in stabilizing the transition state complex. This model is consistent with the long held idea of Pauling (1946) that enzymes work to stabilize the transition state of their reactions. It seems possible that the γ-OH at position 16 could move during the reaction to stabilize the Mg^{2+} during its transition from the γ-, β-phosphates to the α-, β-phosphates. In support of this conjecture, such a role has been proposed for an aspartic acid in the transition of the metal ion of xylose isomerase (Van Tilbeurgh et al., 1992).

Additional evidence for placement of the γ-OH group of amino acid 16 of FeP in association with the Mg^{2+} of the bound nucleotide comes from the X-ray structural analysis of the MgGTP-binding ras p-21 protein and the elongation factor EF-Tu. Several lines of evidence, including high-resolution X-ray data (Milburn et al., 1990) and EPR data (Tong et al., 1991; Latwesen et al., 1992), reveal that a serine of ras p-21, which is equivalent to serine 16 of FeP_{Av}, is a first sphere ligand to the Mg^{2+}. In fact, for ras p-21, this serine is the only protein ligand to the Mg^{2+}, the other ligands being the phosphates of MgGTP and four H_2O molecules (Latwesen et al., 1992). The X-ray structure of EF-Tu likewise suggests that a threonine, equivalent to our serine 16, interacts with the Mg^{2+} of the bound nucleotide (Kjeldgaard & Nyborg, 1992).

Changing the serine at position 16 of the FeP to a threonine results in an increased stability of the FeP·MgATP complex as evidenced by the lower K_m for MgATP. Because threonine differs from serine in the replacement of the γ-H of Ser with the larger γ-CH_3 group of Thr, one might predict that the γ-CH_3 group would restrict the rotation of the γ-OH group. It is suggested then that the γ-CH_3 group forces the γ-OH-group of threonine nearer to the Mg^{2+} in the MgATP-bound state, with the result being greater stability for the FeP·MgATP complex (i.e., lower K_m) and at the same time a reduced stability for the transition-state species, as suggested by the lowered k_{cat} of the T16 FeP.

A similar line of reasoning could be used to explain the differences in activity of the threonine and serine FePs toward Mn^{2+}, which has a larger ionic radius than Mg^{2+}. In this case, when compared with the Mg^{2+}, the γ-CH_3 group of threonine would further hinder the movement of the Mn^{2+} to the transition-state or product-state positions, accounting for the major decrease in the rate of

MnATP hydrolysis by the threonine-containing FeP when compared with the rate of the serine-containing FeP.

Physiological significance

All 22 FePs examined to date have serine at position 16 (Normand & Bousquet, 1989). In other families of nucleotide-binding proteins whose functions are different from that of nitrogenase, both threonine and serine are used at the equivalent positions. Because threonine at position 16 of the FeP results in an FeP with greater catalytic efficiency toward MgATP, then why is threonine not used naturally in FePs? The most likely answer to this question can be found in an examination of the concentration of MgATP within the cell and the need to regulate nitrogenase activity. Nitrogen fixation is a very costly process, utilizing about 16 MgATP per N_2 reduced, and control of this reaction is required by the cell to prevent exhaustion of ATP. It has been proposed that enzymes have evolved with K_m's slightly higher than the cellular concentration of the substrate, thus providing sensitive regulation of activity (Fersht, 1974; Fersht & Wilkinson, 1985). In line with this argument, *A. vinelandii* has been shown to have a total internal MgATP concentration of about 2.3 mM (Upchurch & Mortenson, 1980), a value similar to other bacterial cells (1 mM for *Escherichia coli*; Mathews, 1972). The MgATP concentration available to nitrogenase obviously is below this value because MgATP also would be bound to other ATP-requiring enzymes. Because the K_m (MgATP) for wild-type FeP is about 200 μM, a free MgATP concentration slightly lower than 200 μM would be predicted to be a reasonable value. This condition would provide nitrogenase with regulation of its utilization of MgATP. In contrast, the S16T FeP, with a K_m (MgATP) 10 times lower than wild-type FeP, would be saturated at cellular concentrations and would provide little control of MgATP utilization.

The cellular concentration of MgADP would also be predicted to play a major role in controlling nitrogenase because MgADP binds competitively with MgATP. Thus, MgADP would be a product regulator of nitrogenase, and because the affinity of S16T FeP for MgADP is the same as for wild-type FeP and its affinity for MgATP is 11-fold greater, it is predicted that for S16T FeP MgADP would be less effective as a competitive inhibitor of MgATP interaction. Thus, although the S16T FeP clearly is more efficient in vitro in MgATP utilization, it would only be an advantage in vivo under energy-deficient conditions.

Materials and methods

Site-directed mutagenesis of nitrogenase FeP

A fragment of *A. vinelandii* chromosomal DNA containing the nitrogenase FeP gene (*nifH*) was amplified by the polymerase chain reaction from a 5.64-kb *Sma*I fragment of pDB6 (Robinson et al., 1987) using synthesized oligonucleotides of sequence 5′-CATGTCTAGAAGGGCAA GAATCGACAAC-3′ and 5′-CGGTGGATCCGGCGCG CGAATACTGGCC-3′. The resulting amplified fragment (1.72 kb) contained the *nifH* gene and about 400 bp of flanking *nif* sequence on both sides. In addition, the above oligonucleotide primers were designed to introduce the new restriction sites *Xba*I at the 5′ end and *Bam*HI at the 3′ end of the 1.72-kb amplified fragment. Following digestion with *Xba*I and *Bam*HI, the 1.72-kb fragment was cloned into the *Xba*I and *Bam*HI sites of the phagemid vector pSELECT-1 (Lewis & Thompson, 1990). The resulting plasmid (pLCS 792) was transformed into *E. coli* strain JM109 for production of single-stranded DNA by infection with the helper phage R408. The single-stranded plasmid was purified as described (Promega, 1991) and was used as a template in marker strand selection site-directed mutagenesis as outlined previously. *NifH* complementary mutagenic oligonucleotides were synthesized by the Molecular Genetics Core Facility of the University of Georgia. The ampicillin repair oligonucleotide was purchased from Promega Corp. (Madison, Wisconsin). Mutations in the *nifH* gene were confirmed by DNA sequencing using Sequenase (US Biochemical, Cleveland, Ohio) and a series of *nifH*-specific oligonucleotides. The mutated forms of *nifH* were integrated into the *A. vinelandii* chromosome by the gene replacement technique previously described (Jacobson et al., 1989a,b).

Cell growth and production of altered FePs

Altered FePs were expressed in the appropriate mutated *A. vinelandii* by the derepression protocol previously outlined (Seefeldt et al., 1992). Growth studies were done by centrifugation of urea-grown cells followed by resuspension in growth media lacking a fixed nitrogen source (Seefeldt et al., 1992).

Purification of nitrogenase FePs

Wild-type and altered FePs were purified essentially as described (Seefeldt et al., 1992) with some modifications. Briefly, 100 g of cell paste were suspended in 50 mM Tris, pH 8.0, buffer with 0.2 mg mL^{-1} deoxyribonuclease and lysed by passage through a French pressure cell. The lysed cells were evacuated and flushed with argon. All subsequent steps were performed in the absence of oxygen with a gas phase of argon and with argon-saturated buffers. The lysed cells were centrifuged at 54,000 × *g* for 1 h to remove cell debris. The supernatant solution was either loaded directly onto the first column or subjected to a heat step at 56 °C for 4 min, followed by centrifugation as above. The supernatant (with or without a heat step) was loaded onto a Q-Sepharose column and proteins were eluted as previously described (Seefeldt et al., 1992). The FeP-containing fractions were concentrated by ultrafiltra-

tion (Amicon concentrator, YM30 membrane) and loaded onto a Sephacryl S-200 high load gel permeation column (2.6 × 60 cm, Pharmacia) equilibrated with 50 mM Tris, pH 8.0, with 500 mM NaCl and developed at a flow rate of 2 mL min^{-1}. The FeP-containing fractions were pooled and diluted with 50 mM Tris, pH 8.0, to a final NaCl concentration less than 150 mM. This diluted sample was loaded onto a Mono Q column (1.6 × 10 cm, Pharmacia) equilibrated with 50 mM Tris, pH 8.0, with 100 mM NaCl at a flow rate of 8 mL min^{-1}. The proteins were eluted with a 20 column volume gradient from 100 mM NaCl to 600 mM NaCl at a flow rate of 8 mL min^{-1}. The FeP-containing fractions were pooled and concentrated as described using ultrafiltration. The FeP was then frozen and subsequently stored in liquid nitrogen. All proteins used were homogeneous as judged by analysis on SDS gels stained with Coomassie blue.

Protein determination, SDS gel electrophoresis, and N-terminal amino acid sequencing

SDS gel analysis of proteins and N-terminal amino acid sequencing of the altered FePs was accomplished as described previously (Seefeldt et al., 1992). Protein was determined by the modified Biuret method (Chromy et al., 1974) using bovine serum albumin as standard.

MgATP- and MgADP-binding assays

The binding of MgATP or MgADP to FePs was measured by an equilibrium binding technique previously described (Seefeldt et al., 1992) with the modification that the nucleotides were separated and quantified by high performance liquid chromatography using a C18 reversed-phase column (4.6 mm × 25 cm; Supelco, Bellefonte, Pennsylvania) developed isocratically with a mobile phase of 0.1 M KH_2PO_4 buffer, pH 6.0, at a flow rate of 1.3 mL min^{-1} (Stocchi et al., 1985). The elution of adenosine di- and triphosphates was monitored by measuring the absorbance at 259 nm using an extinction coefficient of 15.4 mM^{-1} cm^{-1}.

Activity assays

Acetylene reduction and H_2 evolution activities were determined using a standard assay mixture as previously described (Seefeldt et al., 1992). For MgATP titration experiments, ATP was not included in the assay mixture, but instead was added to the reaction vials from a stock solution of ATP. For assays in the presence of low salt, the assay mixture contained 2.0 mM ATP, 2.5 mM $MgCl_2$, 6 mM creatine phosphate, 0.125 mg mL^{-1} creatine phosphokinase, 10 mM dithionite, 1.25 mg mL^{-1} BSA, and 25 mM Tris, pH 8.0 (Deits & Howard, 1990). For Mg^{2+} and Mn^{2+} titration experiments, Mg^{2+} was not included in the low salt assay mixture. Instead, either $MgCl_2$ or $MnCl_2$ were added to each assay vial to the indicated concentration from a known stock solution. MgATP hydrolysis activity was determined as described previously (Seefeldt, 1992) except that adenosine tri- and diphosphates were separated and quantified as described above under *MgATP- and MgADP-binding assays*. N_2 reduction activity was determined by quantitation of NH_3 in the assay mixture using a modification of the Conway microdiffusion assay (Mortenson, 1961).

MgATP-induced conformational effects

The MgATP-dependent chelation of Fe^{2+} from FeP was monitored as previously described (Seefeldt et al., 1992) using the formation of the colored complex of Fe^{2+}-α,α'-dipyridyl and its extinction coefficient of 8,400 M^{-1} cm^{-1} at 520 nm. Samples for EPR were prepared and spectra were recorded as previously described (Seefeldt et al., 1992).

Acknowledgments

We thank W.W. Cleland, University of Wisconsin-Madison, for the analysis of the binding constants in Figure 2. We also thank Dr. T.V. Morgan for helpful discussions and Sandra Gay, Judith Adams, Pam Mortenson, and Rita Hayes for technical assistance. This work was supported by National Institutes of Health grant R01-GM40067.

References

Bolin, J.T., Ronco, A.E., Mortenson, L.E., Morgan, T.V., Williamson, M., & Xuong, N.H. (1990). Structure of the nitrogenase MoFe protein: Spatial distribution of the intrinsic metal atoms determined by X-ray anomalous scattering. In *Nitrogen Fixation: Achievements and Objectives* (Gresshoff, P.M., Roth, L.E., Stacey, G., & Newton, W.E., Eds.), pp. 117-122. Chapman & Hall, New York.

Bui, P.T. & Mortenson, L.E. (1968). The hydrolysis of adenosine triphosphate by purified components of nitrogenase. *Biochemistry 8*, 2462-2465.

Burgess, B.K. (1990). The iron-molybdenum cofactor of nitrogenase. *Chem. Rev. 90*, 1377-1406.

Burns, R.C. (1969). The nitrogenase system from *Azotobacter*: Activation energy and divalent cation requirement. *Biochim. Biophys. Acta 171*, 253-259.

Chromy, V., Fischer, J., & Kulhanek, V. (1974). Re-evaluation of EDTA-chelated biuret reagent. *Clin. Chem. 20*, 1362-1363.

Cohn, M. & Hughes, T.R. (1962). Nuclear magnetic resonance spectra of adenosine di- and triphosphate. *J. Biol. Chem. 237*, 176-181.

Deits, T.L. & Howard, J.B. (1990). Effect of salts on *Azotobacter vinelandii* nitrogenase activities. *J. Biol. Chem. 265*, 3859-3867.

Dilworth, M.J. (1966). Acetylene reduction by nitrogen-fixing preparations from *Clostridium pasteurianum*. *Biochim. Biophys. Acta 127*, 285-294.

Fersht, A.R. (1974). Catalysis, binding and enzyme-substrate complementarity. *Proc. R. Soc. Lond. 187*, 397-407.

Fersht, A.R. & Wilkinson, A.J. (1985). Fine structure-activity analysis of mutations at position 51 of tyrosyl-tRNA synthetase. *Biochemistry 24*, 5858-5861.

Georgiadis, M.M., Chakrabarti, P., & Rees, D.C. (1990). Crystal structure of the nitrogenase iron protein from *Azotobacter vinelandii*. In *Nitrogen Fixation: Achievements and Objectives* (Gresshoff, P.M., Roth, L.E., Stacey, G., & Newton, W.E., Eds.), pp. 111-116. Chapman and Hall, New York.

Hageman, R.V. & Burris, R.H. (1978). Nitrogenase and nitrogenase reductase associate and dissociate with each catalytic cycle. *Proc. Natl. Acad. Sci. USA 75*, 2699-2702.

Hausinger, R.P. & Howard, J.B. (1983). Thiol reactivity of the nitrogenase Fe-protein from *Azotobacter vinelandii*. *J. Biol. Chem. 258*, 3486-3492.

Howard, J.B., Davis, R., Moldenhauer, B., Cash, V.L., & Dean, D. (1989). Fe-S cluster ligands are the only cysteines required for nitrogenase Fe-protein activities. *J. Biol. Chem. 264*, 11270-11274.

Jacobson, M.R., Brigle, K.E., Bennett, L.T., Setterquist, R.A., Wilson, M.S., Cash, V.L., Beynon, J., Newton, W.E., & Dean, D.R. (1989a). Physical and genetic map of the major *nif* gene cluster from *Azotobacter vinelandii*. *J. Bacteriol. 171*, 1017-1027.

Jacobson, M.R., Cash, V.L., Weiss, M.C., Laird, N.F., Newton, W.E., & Dean, D.R. (1989b). Biochemical and genetic analysis of the *nifUSVWZM* cluster from *Azotobacter vinelandii*. *Mol. Gen. Genet. 219*, 49-57.

Kjeldgaard, M. & Nyborg, J. (1992). Refined structure of elongation factor EF-Tu from *Escherichia coli*. *J. Mol. Biol. 223*, 721-742.

Latwesen, D.G., Poe, M., Leigh, J.S., & Reed, G.H. (1992). Electron paramagnetic resonance studies of a *ras* p21-Mn^{II}GDP complex in solution. *Biochemistry 31*, 4946-4950.

Lewis, M.K. & Thompson, D.V. (1990). Efficient site directed in vitro mutagenesis using ampicillin selection. *Nucleic Acids Res. 18*, 3439-3443.

Lowe, D.J. & Thorneley, R.N.F. (1984). The mechanism of *Klebsiella pneumoniae* nitrogenase action. *Biochem. J. 224*, 895-901.

Mathews, C.K. (1972). Biochemistry of deoxyribonucleic acid-defective amber mutants of bacteriophage T4. *J. Biol. Chem. 247*, 7430-7438.

Milburn, M.V., Tong, L., deVos, A.M., Brunger, A., Yamaizumi, Z., Nishimura, S., & Kim, S.-H. (1990). Molecular switch for signal transduction: Structural differences between active and inactive forms of protooncogenic *ras* proteins. *Science 247*, 939-945.

Morgan, T.V., Prince, R.C., & Mortenson, L.E. (1986). Electrochemical titration of the S=3/2 and S=1/2 states of the iron protein of nitrogenase. *FEBS Lett. 206*, 4-8.

Mortenson, L.E. (1961). A simple method for measuring nitrogen fixation by cell-free enzyme preparations of *Clostridium pasteurianum*. *Anal. Biochem. 2*, 216-220.

Moustafa, E. & Mortenson, L.E. (1967). Acetylene reduction by nitrogen-fixing extracts of *Clostridium pasteurianum*: ATP requirement and inhibition by ADP. *Nature 216*, 1241-1242.

Muller, C.W. & Schulz, G.E. (1992). Structure of the complex between adenylate kinase from *Escherichia coli* and the inhibitor Ap5A refined at 1.9 Å resolution. *J. Mol. Biol. 224*, 159-177.

Normand, P. & Bousquet, J. (1989). Phylogeny of nitrogenase sequences in *Frankia* and other nitrogen-fixing microorganisms. *J. Mol. Evol. 29*, 436-447.

Pai, E.F., Krengel, U., Petsko, G.A., Goody, R.S., Kabsch, W., & Wittinghofer, A. (1990). Refined crystal structure of the triphosphate conformation of H-*ras* p21 at 1.35 Å resolution: Implication for the mechanism of GTP hydrolysis. *EMBO J. 9*, 2351-2359.

Pauling, L. (1946). Molecular architecture and biological reactions. *Chem. Eng. News 24*, 1375-1377.

Promega Corp. (1991). *Promega Protocols and Applications Guide*. Promega Corp., Madison, Wisconsin.

Robinson, A.C., Dean, D.R., & Burgess, B.K. (1987). Iron-molybdenum cofactor biosynthesis in *Azotobacter vinelandii* requires the iron protein of nitrogenase. *J. Biol. Chem. 262*, 14327-14332.

Saraste, M., Sibbald, P.R., & Wittinghofer, A. (1990). The P-loop—A common motif in ATP- and GTP-binding proteins. *Trends Biol. Sci. 15*, 430-434.

Seefeldt, L.C., Morgan, T.V., Dean, D.R., & Mortenson, L.E. (1992). Mapping the site(s) of MgATP and MgADP interactions with the nitrogenase of *Azotobacter vinelandii*: Lysine 15 of the iron protein plays a major role in MgATP interaction. *J. Biol. Chem. 267*, 6680-6688.

Stocchi, V., Cucchiarini, L., Magnani, M., Chiarantini, L., Palma, P., & Crescentini, G. (1985). Simultaneous extraction and reverse-phase high-performance liquid chromatographic determination of adenine and pyridine nucleotides in human red blood cells. *Anal. Biochem. 146*, 118-124.

Tong, L., DeVos, A.M., Milburn, M.V., & Kim, S.H. (1991). Crystal structure at 2.2 Å resolution of the catalytic domains of normal *ras* protein and an oncogenic mutant complexed with GDP. *J. Mol. Biol. 217*, 503-516.

Upchurch, R.G. & Mortenson, L.E. (1980). *In vivo* energetics and control of nitrogenase fixation: Changes in the adenylate energy charge and adenosine 5'- diphosphate/adenosine 5'-triphosphate ratio of cells during growth on dinitrogen versus growth on ammonia. *J. Bacteriol. 143*, 274-284.

Van Tilbeurgh, H., Jenkins, J., Chiadmi, M., Janin, J., Wodak, S.J., Mrabet, N.T., & Lambeir, A.-M. (1992). Protein engineering of xylose (glucose) isomerase from *Actinoplanes missouriensis*. 3. Changing metal specificity and the pH profile by site-directed mutagenesis. *Biochemistry 31*, 5467-5471.

Walker, J.E., Saraste, M., Runswick, M.J., & Gay, N.J. (1982). Distantly related sequences in the α- and β-subunits of ATP synthase, myosin, kinases and other ATP-requiring enzymes and a common nucleotide binding fold. *EMBO J. 1*, 945-951.

Walsh, C. (1979). *Enzymatic Reaction Mechanisms*. W.H. Freeman, San Francisco.

Wolle, D., Kim, C.-H., Dean, D., & Howard, J.B. (1992). Ionic interactions in the nitrogenase complex: Properties of Fe-protein containing substitutions for Arg-100. *J. Biol. Chem. 267*, 3667-3673.

Yates, M.G. (1991). The enzymology of molybdenum-dependent nitrogen fixation. In *Biological Nitrogen Fixation* (Stacey, G., Burris, R.H., & Evans, H.J., Eds.), pp. 685-735. Chapman and Hall, New York.

Zumft, W.G., Mortenson, L.E., & Palmer, G. (1974). Electron-paramagnetic resonance studies on nitrogenase. *Eur. J. Biochem. 46*, 525-535.